



Design of laser welding applied to T joints between steel and aluminium

Sonia Meco^{a,*}, Supriyo Ganguly^a, Stewart Williams^a, Norman McPherson^b

^a Welding Engineering and Laser Processing Centre, Cranfield University, University Way, United Kingdom

^b University of Strathclyde, 16 Richmond Street, Glasgow, G1 1XQ, Scotland, United Kingdom



ARTICLE INFO

Associate Editor: C.H. Caceres

Keywords:

Dissimilar metal joining
Laser welding
Joint design
Intermetallic compounds
T joint
Steel
Aluminium

ABSTRACT

Laser conduction welding was used to directly join DH36 steel to AA5083 aluminium alloy in a T joint configuration, each plate with 6 mm of thickness. The effect of the process energy (via power density and interaction time) on the joint integrity and quality in terms of cracking, porosity and intermetallic compound layer formation was investigated. Successful T joints were produced by melting of the aluminium plate, which was inserted into a 4 mm deep groove machined on the steel plate, with the heat generated by the laser irradiation on the steel surface. The IMC layer thickness was less than 5 μm . Although cracking was observed along the IMC layer with higher levels of energies, the joints were still strong due to the mechanical inter-locking effect resulting from the novel design of the component, whereby the IMCs were subjected to compressive state of stress while loading.

1. Introduction

The research in dissimilar metal joining of steel to aluminium is mainly focused on thin gauge materials for applications in automotive industry. Applications requiring joining of 6 mm thick plates of steel and aluminium, for instance shipbuilding, such research is quite limited. The current solution to permanently join thick sections of steel and aluminium is to use a transition bar, proprietary name Triclad[®] bar. The half steel and half aluminium Triclad[®] bar is produced by explosion bonding. [Pl \(1989\)](#) explain how the transition bar is produced and how it can be used. This bar permits joining of steel substrate to the steel side and similarly the aluminium substrate to the aluminium side by fusion welding the component. Even though this design solution overcomes the loss in strength by avoiding formation of intermetallic compounds (IMCs), there are a few disadvantages. The application of the transition joint is not cost effective, as it increases the cost of production via the cost of the bar and more complicated logistics of operation from the additional supply chain of this bar. In addition, four fillet welds are necessary when a transition joint is used, instead of two, if steel and aluminium were joined directly. Moreover, there are also issues in joining longitudinally the Triclad[®] bars such as misalignments and distortion and the growth of IMCs within the transition joint. [Tricarico et al. \(2009\)](#) and [Tricarico and Spina \(2010\)](#) investigated the effect of the heat produced during the joining process on the IMC layer growth. [Tricarico et al. \(2009\)](#) used different heat treatments to simulate laser

welding whereas [Tricarico and Spina \(2010\)](#) laser welded the transition bars. Both concluded that the heat of the process enhances the growth of the IMCs.

[Thomas et al. \(2006\)](#) explains that stir-lock is an alternative technique to join dissimilar metals with thick sections. Countersunk holes are machined in the harder material (transition joint) and the softer material is deformed to fill the countersunk holes by friction stir welding, creating a mechanical interlock which gives strength to the joint. The authors claimed to have achieved promising results.

Many studies have been carried out to understand and avoid the formation of IMCs in dissimilar alloys, in particular steel to aluminium. These compounds result from lack of solid solubility between the participating dissimilar alloys. The brittle behaviour of the IMCs is known to be the main reason for the poor mechanical strength of dissimilar metal joints. To minimize the formation and growth of the IMCs, which is a diffusion controlled process, the energy of the joining process must be controlled to minimize the mixing of the metals and reduce the thermal cycle. The solid state joining processes (e.g. explosion bonding and friction stir welding (FSW)) avoid high temperatures and avoid fully molten material so IMCs do not form. However, some of the limitations of the solid state joining processes are the lack of flexibility in terms of joint geometry, material thickness (usually only applied in thin sections) and tool wear as observed in FSW. The fusion based joining processes (e.g. resistance spot welding and laser-MIG (Metal Inert Gas) hybrid welding) cause melting of at least one of the metals and

* Corresponding author.

E-mail addresses: s.a.martinsmeco@cranfield.ac.uk (S. Meco), s.ganguly@cranfield.ac.uk (S. Ganguly), s.williams@cranfield.ac.uk (S. Williams), norman.mcpherson@strath.ac.uk (N. McPherson).

<https://doi.org/10.1016/j.jmatprotec.2019.01.003>

Received 21 November 2017; Received in revised form 11 December 2018; Accepted 3 January 2019

Available online 07 January 2019

0924-0136/ © 2019 The Authors. Published by Elsevier B.V. This is an open access article under the CC BY license (<http://creativecommons.org/licenses/by/4.0/>).

Table 1
Chemical composition of the base metals.

Material	Elements (wt. %)												
	Al	Fe	C	Si	Mn	P + S	Ni	Ti	Cu	Mg	Zn	Cr	Nb
DH36	0.035	Bal.	0.14	0.39	1.37	0.025	0.017	0.002	0.010	–	–	0.018	0.031
5083-H22	Bal.	0.400	–	0.400	0.500	–	–	0.150	0.100	2.600-3.600	0.200	0.300	–

Table 2
Mechanical properties of the steel DH36 (standard ASTM A131:Part 4) and aluminium 5083-H22 (Metalweb, 2013).

Material	Yield strength [MPa]	Ultimate tensile strength [MPa]	Total elongation [%] (at 50 mm of gauge length)
DH36	355	490 - 620	22
5083-H22	250	337	8

therefore, the temperatures involved in the process are much higher, and in most of the cases in fusion welding, the overall thermal cycle is much larger.

There are a few exceptions where fusion based joining processes were successfully used to join steel to aluminium. By controlling the relative position of the heat source in relation to the joint interface and adding filler metal it is possible to avoid melting of the substrate, minimize the reaction between the Fe and Al and create less IMCs. Successful lap-welded joints of 1.2 mm thick hot-dip aluminized (Al-coated) steel to 1.0 mm thick AA5052 aluminium alloy were produced using this technique and a variant of GMAW process, called cold metal transfer (CMT). Kang and Kim (2015) produced joints using magnesium based filler wire and found that the joint strength was equal to that of the heat-affected zone of the aluminium substrate.

Meco et al. (2014) tried to minimize the reaction between Fe and Al by joining steel to aluminium in a lap joint configuration with 2 mm thick steel positioned on the top of 6 mm thick aluminium. Laser conduction welding was used and the process energy was controlled to allow the heat to flow downwards towards the aluminium, without melting the entire thickness of the steel. In this study the Fe-Al IMC layer thickness and the bonding area were correlated to the mechanical strength of the joints for different laser welding conditions. The IMC layer thickness was in the range of 4 and 29 μm and the maximum tensile shear load of the lap joints was over 500 $\text{N}\cdot\text{mm}^{-1}$. In this work the aim is to investigate direct joining of steel to aluminium in a T joint configuration to avoid the use of transition joining systems. A similar welding technique to that used by Meco et al. (2014) and an innovative joint design were applied to the present work. The effect of the process energy, via power density and interaction time, on the joint integrity and quality in terms of cracking, porosity and IMC layer formation was investigated.

2. Experimental procedure

2.1. Material

Low-carbon steel (grade DH36) and AA5083-H22 aluminium alloy plates with 6 mm thickness were used. Both materials are normally used as structural alloys in shipbuilding. The chemical composition and mechanical properties of the materials are given in Tables 1 and 2 respectively. The plate dimensions were 250 mm long and 200 mm wide.

Before welding the steel plates were ground to remove the coating protection and degreased with acetone, whereas the aluminium plates were ground to remove the oxide layer (alumina) and cleaned with ethanol.

A milling machine was used to produce a 6.2 mm wide and 4.0 mm deep groove at the centre of each steel plate, into which the aluminium plate was inserted. A tolerance of 200 μm was chosen for the groove width to allow close tolerance between the plate and the groove and also to consider any variation in plate thickness.

2.2. Laser welding of T joints between steel and aluminium

Laser conduction welding of steel to aluminium in a lap joint configuration was previously studied by Meco et al. (2014) and Pardal et al. (2014), the former used seam welds to join the metals and the latter spot welds. In both studies successful results were achieved. The welding parameters were chosen so that the steel remained solid at the joint interface and only the aluminium was melted during the process, as represented in Fig. 1. In this work an identical joining principle was applied to the T joint configuration (Fig. 1).

To transfer the process developed in a lap joint configuration to the new T joint configuration, it was necessary to take into consideration the joint design. The T joint design should allow the weld to be done with the laser irradiated on a 2 mm thick steel surface in conduction mode, allowing the heat to diffuse through the steel, to melt the aluminium and wet the steel surface. Moreover, the brittle IMC layer formed at the interface of a T joint should not affect the integrity of the joint if the structural stress experienced by the joint on loading is not wholly tensile. Tsumarev et al. (2014) investigated the distribution of the magnitude and type of stresses developed during tensile testing in different joint designs of brazed T joints. The authors showed that the maximum stresses on the brazed joint were 48% lower when the vertical plate was inserted in a rectangular groove machined in the horizontal plate than when a standard T joint was used.

A clamping system, shown in Fig. 2, was also designed and built to permit the laser to irradiate the top of the steel plate and produce a

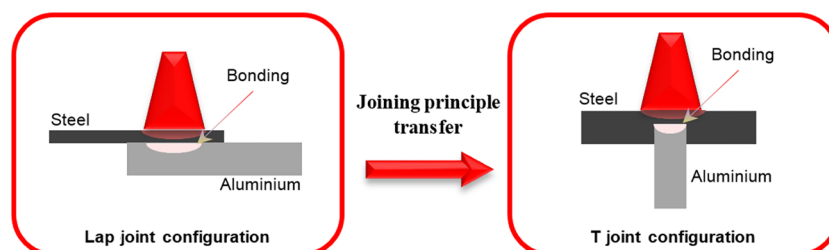


Fig. 1. Schematic representation of laser conduction welding of steel to aluminium transfer from lap-joint to T joint configuration.

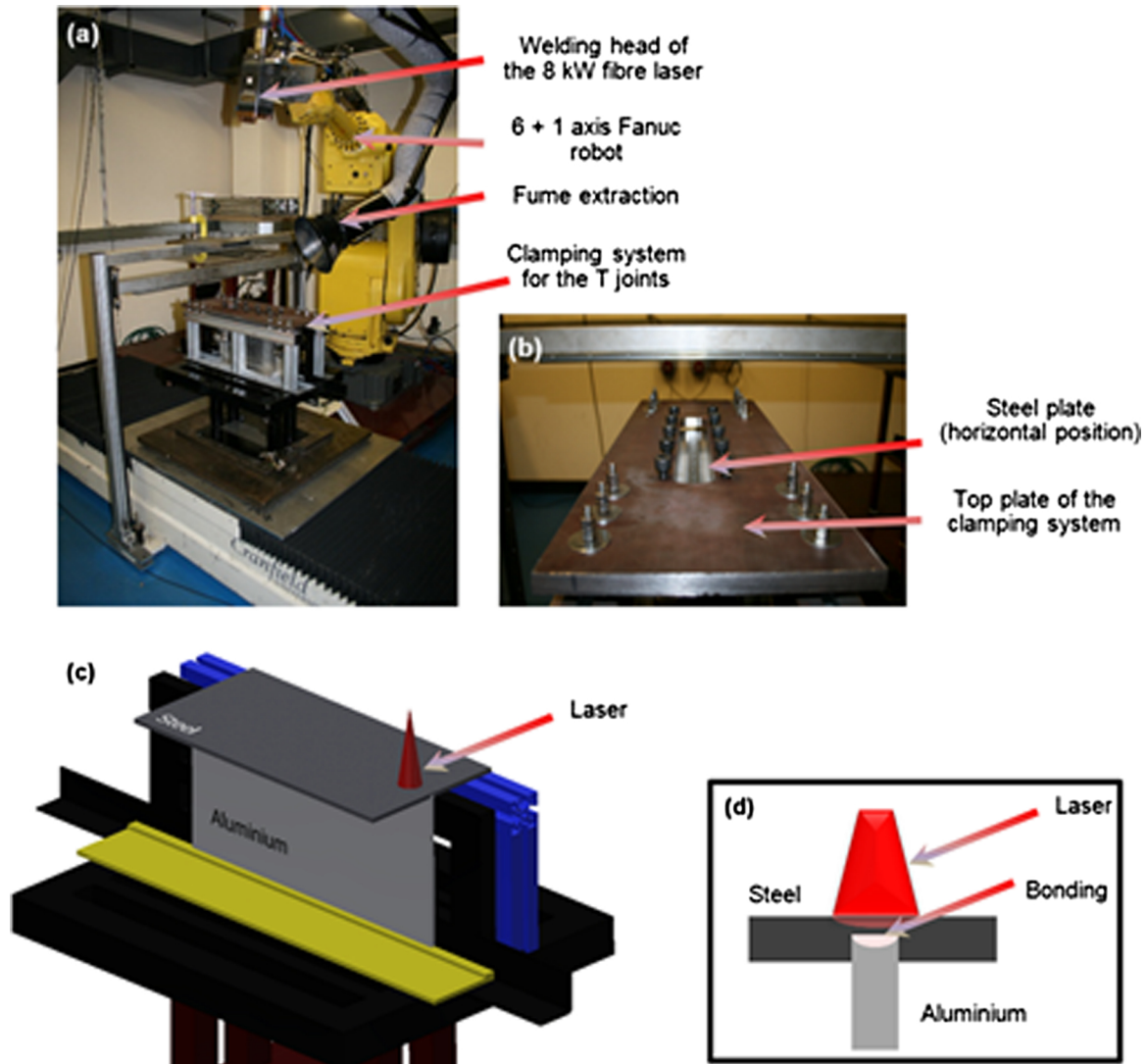


Fig. 2. Experimental setup for laser welding of steel to aluminium in a T joint configuration. (a) General view of the setup, (b) top view of the clamping system, (c) schematic representation of the substrate positioned on the clamping system and (d) schematic representation of the welding process.

seam weld along the plate between the steel and the aluminium. The bolts were tightened with a torque wrench along the top plate to ensure constant pressure along the joint and virtually zero gap between the steel and the aluminium plates which was important for an effective heat transfer from the steel to the aluminium plate.

As previously, no shielding gas nor welding flux were used. The welding flux would create a thermal barrier between the steel and the aluminium plates which could be detrimental to the joining process.

An IPG continuous wave fibre laser with 8000 W of maximum power was used in this work. All the tests were carried out with constant and defocused laser beam of 13 mm diameter and Gaussian intensity distribution (TEM_{00}). The intensity distribution, spot size and divergence of the laser beam were measured using a Primes GmbH focus monitor system. The welding parameters chosen to form the T joints were based on the work from Meco et al. 2017, with identical specific point energy but higher power density.

Meco et al. (2017) found that to achieve optimum joint strength a balance between IMC layer thickness and bonding area is required. A process model was developed which predicted the thermal cycles experienced by the joint and substrate alloys under different laser processing conditions. The model showed that the laser power density is the main factor which determines the peak temperature, as compared to the interaction time. It was also observed that, although a higher peak

temperature would lead to formation of thicker IMC layer, it also results into a larger bonding area, which enhances mechanical strength of the joint. The fundamental laser material interaction parameters (FLMIP), including power density (Eq. (1)), interaction time (Eq. (2)) and specific point energy (Eq. (3)) were used in this work. The FLMIP were previously investigated by Suder and Williams (2012) and Williams and Suder (2011) in autogenous laser welding of similar materials. However, using this approach, these parameters were shown to be effective in controlling the IMC layer thickness and therefore, the joint strength.

$$\text{Power density, PD, MW. m}^{-2} \quad PD = P \cdot A_{beam}^{-1} \quad (1)$$

$$\text{Interaction time, } t_i, \text{ s} \quad t_i = D_{beam} \cdot TS^{-1} \quad (2)$$

$$\text{Specific point energy, } E_{sp}, \text{ kJ} \quad E_{sp} = PD \times t_i \times A_{beam} \quad (3)$$

Where P is laser power, TS is travel speed, D_{beam} and A_{beam} is laser spot diameter and area, respectively.

The welding parameters used in this study are given in Table 3 One sample was produced per experimental condition.

2.3. Metallurgical characterization

For macrostructure and microstructure observations of the joint,

Table 3
Laser welding parameters for joining Fe-Al T joints with a 13 mm laser beam diameter.

Test no.	System parameters		Fundamental material interaction parameters		
	Laser power, kW	Travel speed, m. min ⁻¹	Power density, MW. m ⁻²	Interaction time, s	Specific point energy, kJ
T5	5.5	0.5	41.4	1.6	8.6
T6	5.0	0.4	37.7	2.0	9.8
T7	5.0	0.3	37.7	2.4	11.8
T8	5.0	0.5	37.7	1.6	7.8
T9	5.5	0.4	41.4	2.0	10.7
T10	6.5	0.5	49.0	1.6	10.1
T11	5.0	0.5	37.7	1.6	7.8
T12	6.5	0.5	49.0	1.6	10.1
T13	5.0	0.3	37.7	2.4	11.8
T14	6.0	0.4	45.2	2.0	11.7
T15	6.0	0.5	45.2	1.6	9.4

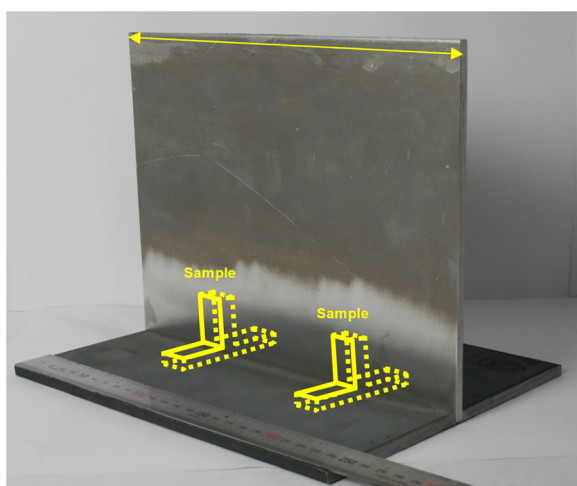


Fig. 3. Schematic representation of the position where the samples for metallographic analysis were machined out from the T joint.

two samples were taken across the 230 mm long weld seam (Fig. 3).

The samples were ground and polished according to standard procedure for optical metallographic analysis. Micrographs of the cross-section were taken with the lowest magnification of the optical microscope (25x) to investigate major defects on the weld, such as porosity or cracking. Microsoft ICE (Image Composite Editor) software was afterwards used to compose the whole macrograph of the T joint (see Fig. 4).

For microstructure analysis nine micrographs were taken across the joint using an optical microscope (400×).

3. Results and discussion

The results presented in this section refer to the cross-sections of the T joints.

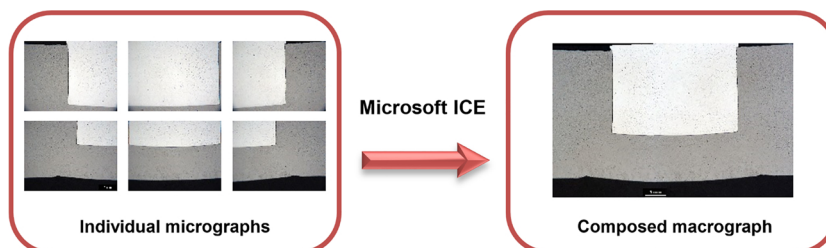


Fig. 4. Composition of individual micrographs into a macrograph using Microsoft ICE software.

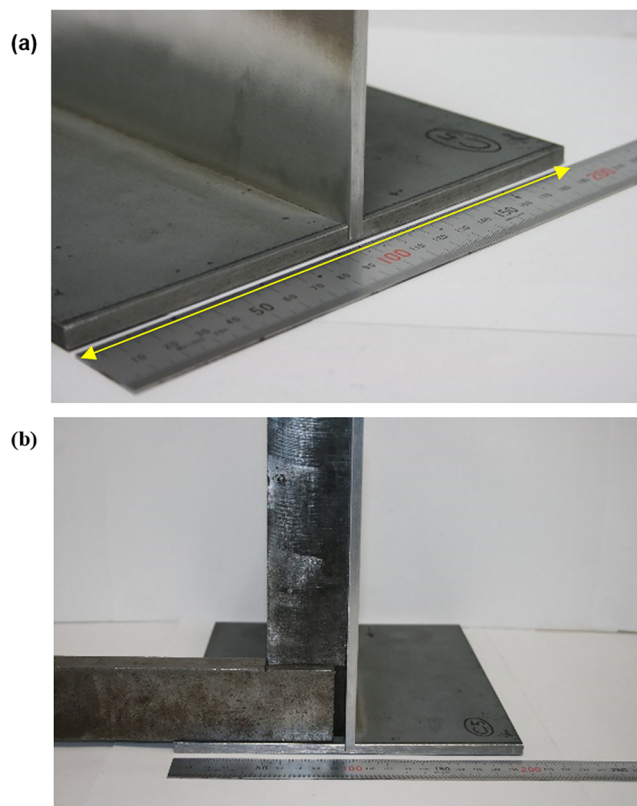


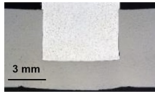
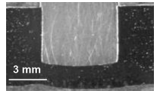
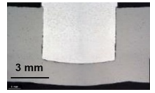
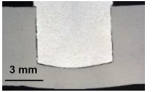
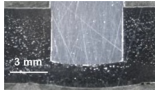
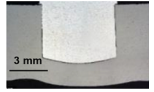
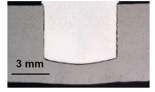
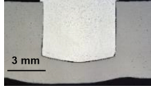
Fig. 5. Images of dissimilar metal Fe-Al T joints after laser welding in (a) perspective view and (b) side view.

3.1. Macrostructural analysis – weld aspects

Laser conduction welding of steel to aluminium has successfully been transferred from the lap joint configuration to the T joint configuration (see Fig. 5). The weld seams along the joints were uniform, no defects were observed and no gaps between the steel and the aluminium were visible. The groove machined on the steel plate seemed to favour the Fe-Al joint strength. A small distortion of the steel plate was observed in all samples after welding causing a beneficial mechanical inter-lock of the aluminium plate. This effect was found to be advantageous to the integrity of the joint since it enhances contact area between the two plates which leads to improved wettability and joint strength.

The macrographs of the different positions of the welded cross sections are shown in Table 4. No porosity was observed in any of the welded specimens. It was also observed that there was more melting at the aluminium plate edge when the specific point energy was higher, either through increasing the power density or the interaction time. For instance, when the joint was produced with $E_{sp} = 7.8$ kJ the edge of the aluminium was completely flat. On the contrary, with higher levels of energy the edge of the aluminium plate became curved and the curvature increased with the applied energy. This indicates a more

Table 4
Cross-sectional view of Fe-Al T joints welded with different welding parameters.

		PD, MW. m ⁻² (P, kW)			
		37.7 (5.0)	41.4 (5.5)	45.2 (6.0)	49.0 (6.5)
t _p , s (TS, m. min ⁻¹)	1.6 (0.5)	 (E _{sp} = 7.8 kJ)	 (E _{sp} = 8.6 kJ)	 (E _{sp} = 9.4 kJ)	 (E _{sp} = 10.1 kJ)
	2.0 (0.4)	 (E _{sp} = 9.8 kJ)	 (E _{sp} = 10.7 kJ)	 (E _{sp} = 11.7 kJ)	-
	2.4 (0.3)	 (E _{sp} = 11.8 kJ)	-	-	-

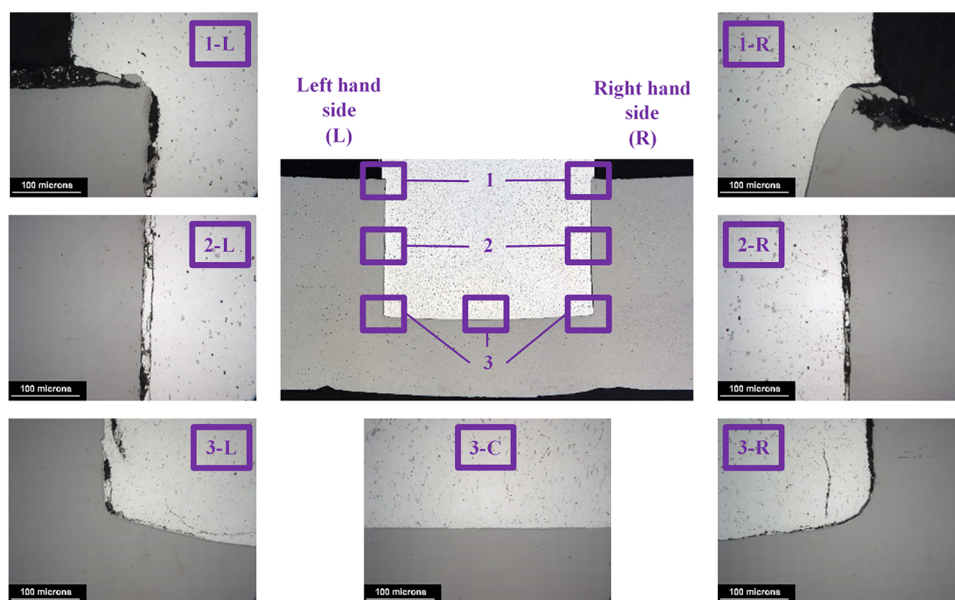


Fig. 6. Micrographs of the Fe-Al interface at different positions - top, middle and bottom lines, at the centre, left and right hand side.

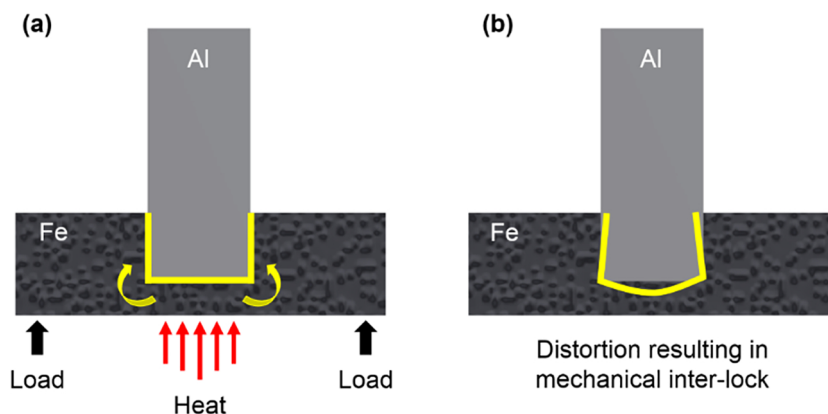


Fig. 7. Schematic representation of the mechanical inter-lock induced during the welding process.

effective wetting of the groove by the molten aluminium which suggests a stronger bonding. However, joints produced with higher level of energy were more susceptible to cracking at the Fe-Al interface. To minimize the differential state of stress at the Fe-Al interface from the

unequal expansion and contraction of the metals, and simultaneously minimize the formation of the IMC and avoiding cracking along the joint interface, processing with lower heat input is recommended.

There was one particular case, corresponding to the joint welded

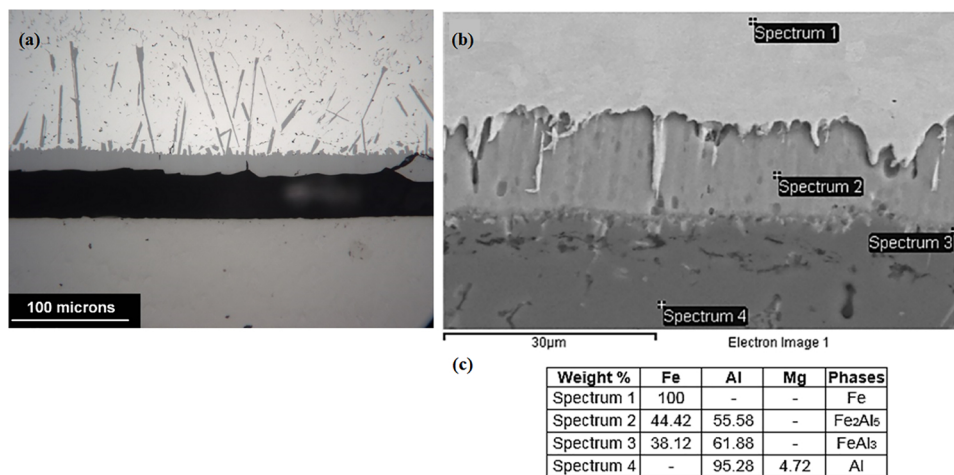
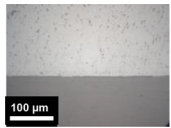
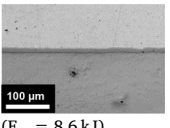
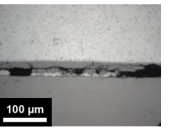
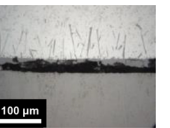
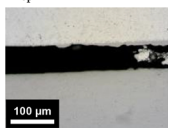
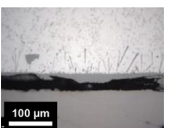
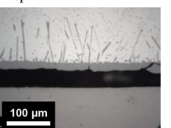
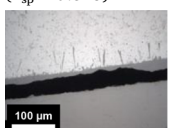


Fig. 8. (a) Optical micrograph of the Fe-Al IMC layer in a T joint and (b–c) EDS spectrum analysis of a lap joint (Meco et al., 2015).

Table 5

Micrographs of the Fe-Al T joints welded with different welding parameters. Micrographs taken at position 3-C which corresponds to the centre of the Fe-Al interface.

		PD, MW. m ⁻² (P, kW)			
		37.7 (5.0)	41.4 (5.5)	45.2 (6.0)	49.0 (6.5)
t _p , s (TS, m. min ⁻¹)	1.6 (0.5)	 (E _{sp} = 7.8 kJ)	 (E _{sp} = 8.6 kJ)	 (E _{sp} = 9.4 kJ)	 (E _{sp} = 10.1 kJ)
	2.0 (0.4)	 (E _{sp} = 9.8 kJ)	 (E _{sp} = 10.7 kJ)	 (E _{sp} = 11.7 kJ)	-
	2.4 (0.3)	 (E _{sp} = 11.8 kJ)	-	-	-

with the minimum energy (E_{sp} = 7.8 kJ), which showed good bonding between the steel and the aluminium (see Fig. 6). At the edge of the aluminium plate where the bonding occurred, there was no cracking (this is observed in Fig. 6 micrograph 3-C). This indicates a sound bonding between the two alloys. The mechanical inter-locking is clear in micrographs 1-L and 1-R of the same figure. A schematic representation of the mechanical inter-lock occurred during the welding process is shown in Fig. 7. The corners of the groove (micrographs 3-L and 3-R) were filled with molten aluminium but there were still small gaps on the sides which require further improvement. A new design of the groove would be recommended to improve the flow of the molten aluminium and thus, improve the bonding between both metals. Lack of fusion/wetting was also observed on the sides of the groove (micrographs 2-L and 2-R in Fig. 6). The small gap between the side of the groove and the aluminium plate forced the molten aluminium to flow upwards by capillarity (micrograph 2-L in Fig. 6). Rapid cooling of the molten aluminium happened when the molten metal touched the colder surface.

3.2. Microstructural analysis – IMC layer

Similar to what was previously observed by Meco et al. (2015) in

laser welding with the plates in lap joint configuration and steel positioned on the top, in the T joint configuration a continuous layer of IMCs was also formed (Fig. 8a). The morphology of the IMC layer is similar to that of the lap joints. The needle shape IMCs are FeAl₃ with 62% Al and the thick tongue shape IMCs are Fe₂Al₅ with 56% Al (Fig. 8b and c). In both joint configurations the energy of the process was controlled to produce partial melting of the steel, away from the Fe-Al interface, and simultaneously melting of the aluminium. Under this condition the reaction between Fe and Al was restricted and the formation of the IMC was minimized.

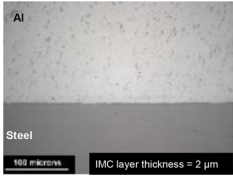
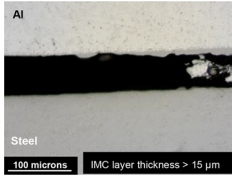
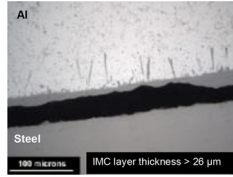


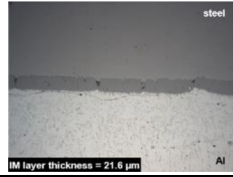
Table 5 shows the micrographs of the IMC layer formed with different levels of applied specific point energy at the Fe-Al interface near to the centre of the weld where the IMC layer has maximum thickness (position 3-C identified in Fig. 6).

The micrographs show that the IMC layer thickness grows as the specific point energy increases, either via power density or interaction time. Similar behaviour was observed by Meco et al. (2015) in laser conduction welding of steel to aluminium in lap joint configuration, where the growth of this layer was studied with the variation of power density, interaction time and specific point energy.

The micrographs in Table 6 permit the comparison of the IMC layers formed in the T joint and lap joint configurations for similar welding

Table 6

Comparison between the IMC layer formed in the lap joint (Meco et al. (2015)) and T joint configuration with similar welding conditions.

T joint configuration		
P = 5 kW		
TS = 0.50 m.min ⁻¹	TS = 0.40 m.min ⁻¹	TS = 0.30 m.min ⁻¹
t _i = 1.6 s PD = 37.7 MW.m ⁻² E _{sp} = 7.8 kJ	t _i = 2.0 s PD = 37.7 MW.m ⁻² E _{sp} = 9.8 kJ	t _i = 2.4 s PD = 37.7 MW.m ⁻² E _{sp} = 11.8 kJ
		
Lap joint configuration		
P = 5 kW		
TS = 0.40 m.min ⁻¹	TS = 0.35 m.min ⁻¹	TS = 0.30 m.min ⁻¹
t _i = 2.0 s PD = 37.7 MW.m ⁻² E _{sp} = 9.8 kJ	t _i = 2.2 s PD = 37.7 MW.m ⁻² E _{sp} = 11.1 kJ	t _i = 2.6 s PD = 37.7 MW.m ⁻² E _{sp} = 13.0 kJ
		

conditions. Even though the IMC layer thickness was not measured in all the T joint samples, due to the crack developed along the IMC layer, it seems that the IMC layer growth follows a similar trend to that found in the lap joints. For both joint configurations, the thickness of the IMC layer of the samples welded with the minimum energy was less than 5 μm. For higher value of energy, the IMC layer is thicker and shows the Fe₂Al₅ layer near the steel (with uniform thickness) and the irregular and needle shape FeAl₃ on the aluminium side as described by Cheng and Wang (2009) in their study about growth of IMC layer in the aluminide mild steel during hot-dipping. However, the FeAl₃ formed in the T joint configuration was more irregular than that observed in the lap joint. This may be due to different cooling rates existent in both joint configurations. In lap joint configuration the contact length between the steel and the aluminium plates is larger than that in the T joint configuration, 46 mm against 6 mm, respectively. Therefore, it is expected that the thermal cycle is more prolonged in the T joint configuration which allows the FeAl₃ phase to grow more.

The micrographs show cracks along the IMC layer only on the T joints. A dissimilar T joint would undergo a tensile-compressive state of stress originating from the differential thermal expansion and contraction under constraint at the joint interface, between the steel and aluminium inside the groove, to which the brittle Fe-Al IMCs failed due to the lack of toughness.

4. Conclusions

- It was possible to transfer the technique of laser welding from lap joint to T joint configuration and still have the solid-liquid joint interface required to form a thin Fe-Al intermetallic compound layer;
- The intermetallic compound layer thickness found on the T joints was similar to that of the lap joints but with more cracking due to tensile-compressive state of stress at the joint interface;
- The new design of the T joint creates a mechanical inter-lock between the steel and the aluminium plates;

- Defect free T joints were produced with minimum power density (37.7 MW.m⁻²) and interaction time (1.56 s). In this case the intermetallic compound layer thickness was less than 5 μm;
- Further investigation of the groove geometry is recommended in order to improve the wetting of molten aluminium on steel inside the groove and reduce cracking;
- This technique seems to be a feasible alternative to the Triclad[®] transition joint. However, mechanical tests should be done to quantify the strength of the laser welded T joints.

Acknowledgements

Dr. Supriyo Ganguly acknowledges the support by Engineering and Physical Sciences Research Council (EPSRC) through grant number EP/J017086/1. Dr. Sonia Meco is grateful to BAE Systems Naval Ships and EPSRC the Centre for Innovative Manufacturing in Laser-based Production Processes (Grant No.: EP/K030884/1) for providing financial support to this project. The underlying data can be accessed through the Cranfield University data repository <https://dx.doi.org/10.17862/cranfield.rd.7673183>.

References

- Cheng, W.J., Wang, C.J., 2009. Growth of intermetallic layer in the aluminide mild steel during hot-dipping. *Surf. Coat. Technol.* 204, 824–828. <https://doi.org/10.1016/j.surfcoat.2009.09.061>.
- Kang, M., Kim, C., 2015. Joining Al 5052 alloy to aluminized steel sheet using cold metal transfer process. *Mater. Des.* 81, 95–103. <https://doi.org/10.1016/j.matdes.2015.05.035>.
- Meco, S., Ganguly, S., Williams, S., McPherson, N., 2014. Effect of laser processing parameters on the formation of intermetallic compounds in Fe-Al dissimilar welding. *J. Mater. Eng. Perform.* 23, 3361–3370. <https://doi.org/10.1007/s11665-014-1106-5>.
- Meco, S., Pardo, G., Ganguly, S., Williams, S., McPherson, N., 2015. Application of laser in seam welding of dissimilar steel to aluminium joints for thick structural components. *Opt. Lasers Eng.* 67, 22–30. <https://doi.org/10.1016/j.optlaseng.2014.10.006>.
- Meco, S., Cozzolino, L., Ganguly, S., Williams, S., McPherson, N., 2017. Laser welding of steel to aluminium: thermal modelling and joint strength analysis. *J. Mater. Process. Technol.* 247, 121–133. <https://doi.org/10.1016/j.jmatprotec.2017.04.002>.

- Metalweb, 2013. Plate, Sheet and Strip Typical Physical Properties - AA5083 H22. [WWW Document]. Alum. Roll. plate sheet. URL. . (Accessed 1 January 15). <http://www.metalweb.co.uk/product/aluminium/aluminium-rolled-plate-sheet/>.
- Pardal, G., Meco, S., Ganguly, S., Williams, S., Prangnell, P., 2014. Dissimilar metal laser spot joining of steel to aluminium in conduction mode. *Int. J. Adv. Manuf. Technol.* 73, 365–373. <https://doi.org/10.1007/s00170-014-5802-y>.
- Pl, P., 1989. Explosion-bonded transition joints for structural applications. *Building* 3, 64–72.
- Suder, W.J., Williams, S.W., 2012. Investigation of the effects of basic laser material interaction parameters in laser welding. *J. Laser Appl.* 24, 032009. <https://doi.org/10.2351/1.4728136>.
- Thomas, W.M., Staines, D.J., Norris, I.M., Westgate, S.A., Wiesner, C.S., 2006. Transition Joints between Dissimilar Materials.
- Tricarico, L., Spina, R., 2010. Experimental investigation of laser beam welding of explosion-welded steel/aluminum structural transition joints. *Mater. Des.* 31, 1981–1992. <https://doi.org/10.1016/j.matdes.2009.10.032>.
- Tricarico, L., Spina, R., Sorgente, D., Brandizzi, M., 2009. Effects of heat treatments on mechanical properties of Fe/Al explosion-welded structural transition joints. *Mater. Des.* 30, 2693–2700. <https://doi.org/10.1016/j.matdes.2008.10.010>.
- Tsumarev, Y.A., Ignatova, Y.V., Tsumarev, Y.N., Latypova, Y.Y., 2014. Reducing the stress concentration in permanent T-joints. *Weld. Int.* 28, 406–408. <https://doi.org/10.1080/09507116.2013.840026>.
- Williams, S., Suder, W., 2011. Use of fundamental laser material interaction parameters in laser welding. *Conference on Lasers and Electro-Optics (CLEO) 2011* 1–2.